J|A|C|S
ARTICLES
Published on Web 01/11/2002

Binding of Hydrophobic Hydroxamic Acids Enhances Peroxidase's Stereoselectivity in Nonaqueous Sulfoxidations

Prasanta Kumar Das, Jose M. M. Caaveiro, Susana Luque,† and Alexander M. Klibanov*

Contribution from the Department of Chemistry, Massachusetts Institute of Technology, Cambridge, Massachusetts 02139

Received August 30, 2001

Abstract: Horseradish peroxidase exhibits a meager stereoselectivity (*E*) in the sulfoxidation of thioanisole (**1a**) in 99.8% (v/v) methanol. The *E* value, however, is greatly enhanced when the enzyme forms a complex with benzohydroxamic acid (**2a**). These findings are rationalized by means of molecular dynamics simulations and energy minimization which correctly explain (i) why the free enzyme is not stereoselective, (ii) why **2a** inhibits peroxidase-catalyzed sulfoxidation of **1a** but the enzymatic formation of one enantiomer of the sulfoxide product is inhibited much more than that of the other, thereby raising peroxidase's *E*, and (iii) why in the presence of **2a** the enzyme favors production of the *S* sulfoxide of **1a**. The generality of the observed ligand-induced stereoselectivity enhancement is demonstrated with other hydrophobic hydroxamic acids, as well as with additional thioether substrates.

Introduction

Improving the stereoselectivity of a given enzyme toward a desired substrate is one of the most challenging but practically important goals in the area of biocatalysis.[1] Conducting enzyme-catalyzed synthetic transformations in organic solvents,[2] instead of conventional aqueous reaction media, offers unprecedented opportunities in this regard.[3] Namely, enzymatic stereoselectivity has been found to be markedly affected by the solvent and by the history/formulation of the enzyme sample.[3] In the present study, we have proposed and validated another, independent approach to that goal.

Peroxidases are a versatile family of redox enzymes capable of catalyzing several asymmetric processes, such as oxidation of prochiral thioethers.[4] The products of this latter process, chiral sulfoxides, are valuable bioactives and synthons.[5] For example, the best-selling drug of all time, anti-ulcer omeprazole (Prilosec/Losec), is such a chiral sulfoxide whose single-enantiomer version is nearing clinical use.[6] Like other enzymatic conversions, peroxidase-catalyzed sulfoxidations often suffer from insufficient stereoselectivity.[4] In this work, we demonstrate that complexation of horseradish peroxidase (HRP) with hydrophobic hydroxamic acids can greatly enhance its stereoselectivity. Moreover, this effect can be correctly rationalized by means of structure-based molecular modeling of the enzyme·substrate and enzyme·substrate·ligand complexes.

Results and Discussion

Peroxidase-catalyzed sulfoxidations and other asymmetric transformations can be carried out not only in water[4] but also, and profitably so, in nearly anhydrous organic solvents.[7] As the initial model reaction, herein we investigated the oxidation of thioanisole (**1a**) catalyzed by lyophilized HRP in

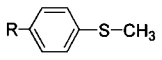

1

1a: R = H
1b: R = $NHCOCH_3$
1c: R = CH_2COOH
1d: R = OCH_3

99.8% (v/v) methanol.[7] Peroxidase-catalyzed sulfoxidation of this prochiral substrate with H_2O_2 lacked stereopreference: the stereoselectivity value $E(S/R)$[8] was found to be 1.1 ± 0.1 (top line in Table 1). The $E(S/R)$ value was only slightly higher, 1.8 ± 0.2, when an alternative oxidant, *tert*-butyl hydroperoxide (*t*-BuOOH), was used (top line in Table 1).

Benzohydroxamic acid (**2a**) is known to bind in the vicinity of the active site's heme of HRP, as well as of other

* Corresponding author. E-mail: klibanov@mit.edu.
† Permanent address: Department of Chemical and Environmental Engineering, University of Oviedo, 33071 Oviedo, Spain.

(1) Faber, K.; Ottolina, G.; Riva, S. *Biocatalysis* **1993**, *8*, 91−132. Margolin, A. L. *Enzyme Microb. Technol.* **1993**, *15*, 266−280. Roberts, S. M.; Turner, N. J.; Willets, N. J.; Turner, M. K. *Introduction to Biocatalysis Using Enzymes and Microorganisms*; Cambridge University Press: New York, 1995. Faber, K. *Biotransformations in Organic Chemistry*, 4th ed.; Springer-Verlag: Berlin, 2000.
(2) Carrea, G.; Riva, S. *Angew. Chem.* **2000**, *33*, 2226−2254.
(3) Klibanov, A. M. *Nature* **2001**, *409*, 241−246.
(4) Van Deurzen, M. P. J.; Van Rantwijk, F.; Sheldon, R. A. *Tetrahedron* **1997**, *53*, 13183−13220. Colonna, S.; Gaggero, N.; Richelmi, C.; Pasta, P. *Trends Biotehchnol.* **1999**, *17*, 163−168. Adam, W.; Lazarus, M.; Saha-Möller, C. R.; Weichold, O.; Hoch, U.; Häring, D.; Schreier, P. *Adv. Biochem. Eng./Biotechnol.* **1999**, *63*, 73−108.
(5) Carreno, M. C. *Chem. Rev.* **1995**, *95*, 1717−1760.
(6) Cannarsa, M. J. *Chim. Oggi/Chem. Today* **1999**, *17* (9), 28−32.
(7) Dai, L.; Klibanov, A. M. *Biotechnol. Bioeng.* **2000**, *70*, 353−357. Xie, Y.; Das, P. K.; Klibanov, A. M. *Biotechnol. Lett.* **2001**, *23*, 1451−1454.
(8) Defined as the ratio of the initial rate for the production of the *S* sulfoxide to that of the *R* sulfoxide in the same reaction mixture. See: Chen, C.-S.; Fujimoto, Y.; Girdaukas, G.; Sih, C. J. *J. Am. Chem. Soc.* **1982**, *104*, 7294−7299. Straathof, A. J. J.; Jongejan, J. A. *Enzyme Microb. Technol.* **1997**, *21*, 559−571.

10.1021/ja012075o CCC: $22.00

Table 1. Initial Rates and Stereoselectivities *E*(*S*/*R*) of the Asymmetric Sulfoxidation of Thioanisole (**1a**) Catalyzed by HRP in the Presence of Varying Concentrations of Benzohydroxamic Acid (**2a**) in 99.8% Methanol[a]

	initial rate of product formation,[b] μM/min					
	with H_2O_2			with *t*-BuOOH		
[**2a**], mM	*S* sulfoxide	*R* sulfoxide	*E*(*S*/*R*)[8]	*S* sulfoxide	*R* sulfoxide	*E*(*S*/*R*)[8]
0	4.0 ± 0.4	3.5 ± 0.2	1.1 ± 0.1	2.4 ± 0.3	1.3 ± 0.2	1.8 ± 0.2
0.5	1.5 ± 0.1	1.1 ± 0.1	1.4 ± 0.1	1.1 ± 0.1	0.45 ± 0.02	2.4 ± 0.2
1.0	0.77 ± 0.06	0.41 ± 0.03	1.9 ± 0.1	0.48 ± 0.04	0.14 ± 0.02	3.4 ± 0.4
2.0[c]	0.49 ± 0.02	0.19 ± 0.01	2.6 ± 0.1	0.46 ± 0.03	0.10 ± 0.01	4.6 ± 0.4[c]
4.0	0.40 ± 0.04	0.13 ± 0.01	3.1 ± 0.3	0.38 ± 0.05	0.076 ± 0.012	5.0 ± 0.7
7.0	0.29 ± 0.02	0.080 ± 0.004	3.6 ± 0.2	0.27 ± 0.03	0.046 ± 0.005	5.9 ± 0.6
10	0.24 ± 0.01	0.060 ± 0.006	4.0 ± 0.3	0.21 ± 0.01	<0.028	>7.1

[a] Lyophilized enzyme powders were suspended in methanol (0.2% water) containing 0.5 mM **1a**, 1 mM peroxide, and **2a**. Each reaction mixture (1 mg/mL of HRP in the case of H_2O_2, and 10 mg/mL in the case of *t*-BuOOH) was vigorously stirred at room temperature; periodically, aliquots were withdrawn and assayed by chiral HPLC, as described in the Methods section. [b] All initial reaction rates were calculated by the least-squares method, with the mean and standard error values shown in the table. [c] For HRP lyophilized from its aqueous solution containing 1 mM **2a** (second paragraph of Results and Discussion) and then suspended in methanol following our experimental protocol, the calculated ligand concentration in that solvent was 2 mM. However, when 2 mM **2a** was directly added to the methanol suspension of HRP lyophilized in the absence of ligand, the *E*(*S*/*R*) value obtained, 4.6 ± 0.4, was below that in the former case (>7.5). This discrepancy suggests that some of the ligand co-lyophilized with HRP becomes trapped in the enzyme sample and thus is not released into the solvent when the lyophilized powder is suspended in methanol.

oxidoreductases, and inhibit the enzyme.[9−11] We decided to explore whether the extent of this inhibition would be identical for the enzymatic formation of *S* and *R* sulfoxides from **1a**. To this end, HRP (5 mg/mL) and **2a** (0.75 mM) were dissolved in a buffered (pH 7.0) aqueous solution, followed by lyophilization. The resultant enzyme·**2a** complex was assayed in the oxidation of **1a** with *t*-BuOOH in 99.8% methanol under the same conditions as the free enzyme above. It was found that while the complexation with the ligand lowered the initial rate of the peroxidase-catalyzed production of the *S* sulfoxide 5.2-fold, that for the *R* enantiomer plummeted 17-fold. Consequently, the stereoselectivity more than trippled—from 1.8 ± 0.2 to 5.7 ± 0.6. The *E*(*S*/*R*) value increased with the concentration of **2a** in the aqueous solution of the enzyme prior to lyophilization: for example, it was merely 3.4 ± 0.2 at the 0.3 mM ligand but exceeded 7.5 for the 1 mM ligand.

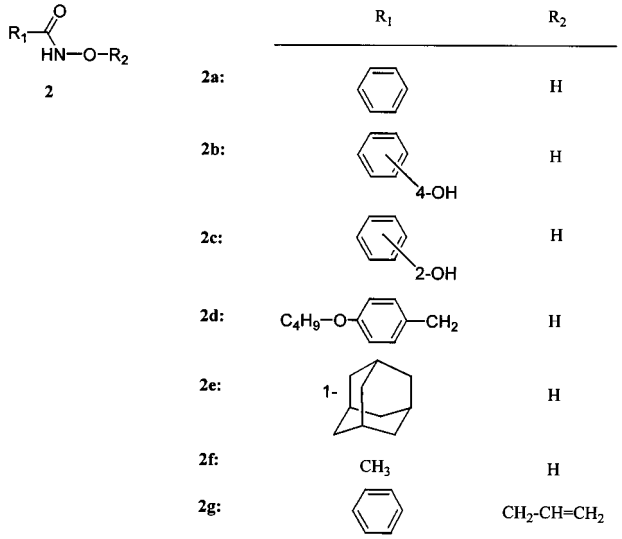

We found that, as in aqueous solution,[9] **2a** is a potent inhibitor of peroxidase's natural reaction (phenol oxidation with H_2O_2)[12] in 99.8% methanol. For instance, addition of 0.5 mM **2a** to the reaction mixture cut the initial rate of the enzymatic oxidation of 0.5 mM *o*-methoxyphenol with 0.1 mM H_2O_2 some 8-fold in that organic solvent. Therefore, we examined whether a direct addition of **2a** to lyophilized HRP suspended in 99.8% methanol will also unequally affect the rates of *S* and *R* sulfoxidations of **1a**, and hence raise stereoselectivity, in a manner similar to that observed in the aforementioned experiments with the preformed, lyophilized enzyme·ligand complex. Inspection of Table 1 indicates that, whether with H_2O_2 or *t*-BuOOH as an oxidant, **2a** added to a mixture of HRP and **1a** in methanol significantly inhibits the formation of both *S* and *R* sulfoxides. Furthermore, in all cases the ligand slows down the production of the *R* enantiomer far more than the *S*, thereby giving rise to an enhanced stereoselectivity. At the highest **2a** concentration used, 10 mM, the *E*(*S*/*R*) value grew from 1.1 ± 0.1 to 4.0 ± 0.3 for H_2O_2 and from 1.8 ± 0.2 to >7.1 for *t*-BuOOH (Table 1), i.e., from un- or barely detectable to quite substantial.

To explain the foregoing observations mechanistically, we employed the means of molecular modeling involving molecular dynamics simulations and energy minimization.[13] Upon reaction with a peroxide, the ferric heme state of peroxidase is converted to the catalytically active compound I, an Fe═O oxyferryl species, which is two oxidation states above the resting state;[14] in the sulfoxidation of thioanisole, the iron-bound oxygen atom is subsequently transferred to the substrate's sulfur atom.[15]

(9) Schonbaum, G. R. *J. Biol. Chem.* **1973**, *248*, 502−511. Maltempo, M. M.; Ohlsson, P. L.; Paul, K. G.; Petersson, L.; Ehrenberg, A. *Biochemistry* **1979**, *18*, 2935−2941. Aviram, I. *Arch. Biochem. Biophys.* **1981**, *212*, 483−490. Kitagawa, T.; Hashimoto, S.; Teraoka, J.; Nakamura, S.; Yajima, H.; Toichiro, H. *Biochemistry* **1983**, *22*, 2788−2792. Sakurada, J.; Takahashi, S.; Hosoya, T. *J. Biol. Chem.* **1986**, *261*, 9657−9662. Smulevich, G.; English, A.; Mantini, A. R.; Marzocchi, M. P. *Biochemistry* **1991**, *30*, 772−779. LaMar, G. N.; Hernández, G.; de Ropp, J. S. *Biochemistry* **1992**, *31*, 9158−9168. Veitch, N. C. *Biochem. Soc. Trans.* **1995**, *23*, 232−240. Itakura, H.; Oda, Y.; Fukuyama, K. *FEBS Lett.* **1997**, *412*, 107−110. de Ropp, J. S.; Mandal, P.; Brauer, S. L.; LaMar, G. N. *J. Am. Chem. Soc.* **1997**, *119*, 4732−4739. Smulevich, G.; Feis, A.; Indiani, C.; Becucci, M.; Marzocchi, M. P. *J. Biol. Inorg. Chem.* **1999**, *4*, 39−47. Indiani, C.; Feis, A.; Howes, B. D.; Marzocchi, M. P.; Smulevich, G. *J. Am. Chem. Soc.* **2000**, *122*, 7368−7376.
(10) Henriksen, A.; Schuller, D. J.; Meno, K.; Welinder, K. G.; Smith, A. T.; Gajhede, M. *Biochemistry* **1998**, *37*, 8054−8060.
(11) Chang, Y.-T.; Veitch, N. C.; Loew, G. H. *J. Am. Chem. Soc.* **1998**, *120*, 5168−5178.
(12) Saunders: B. C.; Holmes-Siedle, A. G.; Stark, B. P. *Peroxidase*; Butterworth: Washington, DC, 1964. Everse, J.; Everse, K. E.; Grisham, M. B., Eds. *Peroxidases in Chemistry and Biology*; CRC Press: Boca Raton, FL, 1991.
(13) Ke, T.; Klibanov, A. M. *J. Am. Chem. Soc.* **1999**, *121*, 3334−3340. Shin, J.-S.; Luque, S.; Klibanov, A. M. *Biotechnol. Bioeng.* **2000**, *69*, 577−583.
(14) Harris, D. L.; Loew, G. H. *J. Am. Chem. Soc.* **1996**, *118*, 10588−10594.
(15) Kobayashi, S.; Nakano, M.; Kimura, T.; Schaap, A. P. *Biochemistry* **1987**, *26*, 5019−5022.

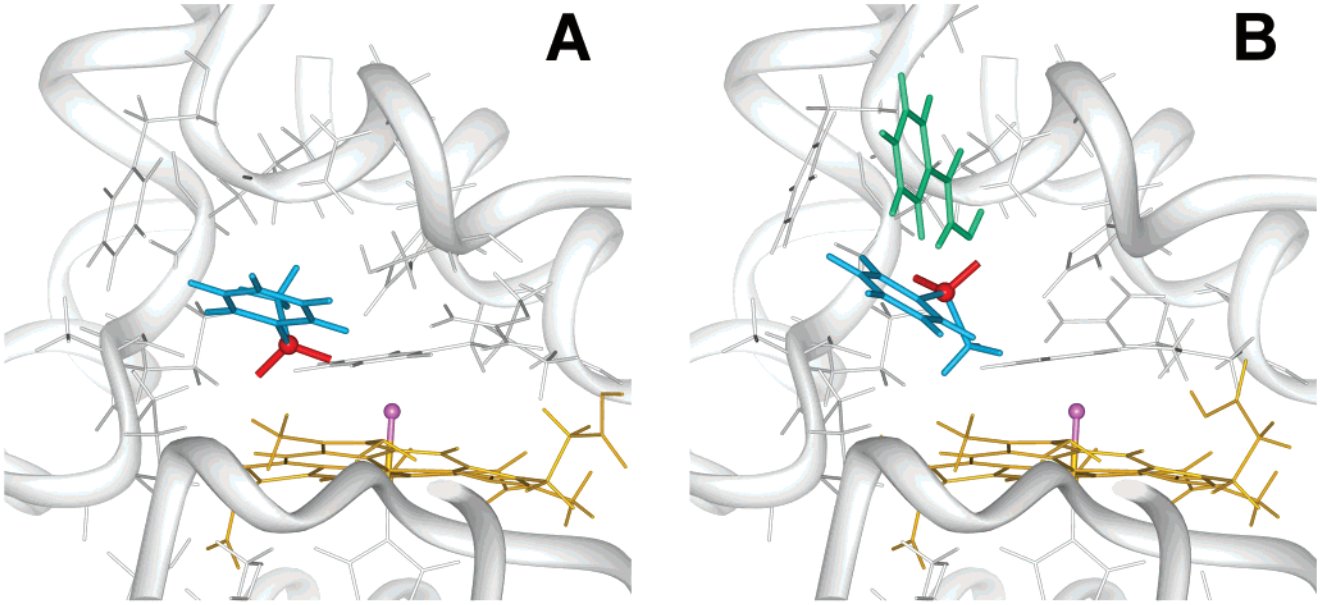

Figure 1. Molecular models of the binary complex of HRP with the substrate **1a** (A) and of the ternary complex of HRP with **1a** and the ligand **2a** (B). The depicted oxyferryl form of the enzyme is capable of transferring its heme-bonded oxygen atom to the **1a**'s sulfur atom to form a chiral sulfoxide. The molecular models were built on the basis of the X-ray crystal structures[10,16] of HRP and its complexes with **2a** and with the natural substrate ferulic acid and cyanide, as described in the Methods section. Representations: a gray ribbon, the protein backbone; black/gray/white sticks, amino acid side chains; golden sticks, the heme; a pink ball, the oxyferryl-heme's oxygen; blue sticks, bound **1a** whose sulfur atom and its two lone pairs of electrons are denoted by a red ball and red sticks, respectively; and green sticks, bound **2a**. For clarity, (i) only the portion of the protein backbone situated within a 15-Å sphere with the center at the substrate's sulfur atom and (ii) the side chains situated within 7 Å from either the sulfur or oxygen atoms (red and pink balls, respectively) are shown.

The starting structure for the modeling of the enzyme·**1a** complex was, therefore, approximated by the recently solved X-ray crystal structure of the ternary complex of HRP with the natural substrate ferulic acid (which we replaced by **1a**) and cyanide (replaced by oxygen).[16] This starting structure was then subjected to molecular dynamics simulations and energy minimization, and the lowest-energy structure thus obtained was chosen as that of the catalytically relevant oxyferryl-peroxidase·**1a** complex.

Figure 1A depicts the extended active site region of the resultant lowest-energy structure. The protein backbone is represented by a ribbon, the heme by golden sticks, the oxyferryl's oxygen atom by a pink ball, **1a** by blue sticks, and **1a**'s sulfur atom and its two lone electron pairs by red ball-and-sticks, respectively. In addition, all amino acid residues' side chains located within 7 Å from either the oxyferryl's oxygen or **1a**'s sulfur are represented by black/white/gray sticks (note that the impression that the benzene ring of Phe41 in the center of Figure 1A is in close proximity of the substrate's S atom is an optical illusion; in actuality, it is way behind the plane of the figure with its closest atom being 3.7 Å away from the sulfur).

In the enzymatic sulfoxidation, the oxyferryl-heme's O is transferred to the bound **1a**'s sulfur to become a co-owner of one of its lone pairs of electrons. If the latter denoted by a red stick pointing southwest in Figure 1A is shared by the oxygen atom, then application of the Cahn−Ingold−Prelog convention[17] yields the *S* enantiomer of the sulfoxide product. Conversely, if the red stick pointing southeast is engaged, the *R* enantiomer ensues. It is apparent from Figure 1A that the sulfur's two lone pairs are similarly accessible to the attacking oxygen atom. Therefore, one would expect comparable concentrations of the *S* and *R* sulfoxides, i.e., no appreciable stereoselectivity. This was indeed observed experimentally, with the *E*(*S*/*R*) values being in the 1 to 2 range depending on the oxidant used (top line of Table 1).

On the basis of kinetic studies, **2a** is generally regarded as a competitive inhibitor of HRP.[9] This view is supported by X-ray crystal structure data: the position occupied by **2a** in its binary complex[10] with the enzyme coincides with that occupied by the natural substrate ferulic acid.[16] However, our observations indicate that at least in the case of enzymatic sulfoxidations this cannot be the whole picture because **2a** should then inhibit the formation of *S* and *R* sulfoxides of **1a** to the same extent. As seen in Table 1, that is clearly not so, with the *R* sulfoxidations being inhibited much more than the *S*.

A recent theoretical study[11] of binding modes of **2a** in the cyanide-ligated (i.e., oxyferryl-mimicking) form of HRP revealed the existence of several secondary ligand binding sites, in addition to the main one coinciding with that for the substrate. Therefore, we set out to build a ternary complex of the oxyferryl form of the enzyme with **1a** and **2a**, whereby the former occupies the previously identified hydrophobic substrate binding site[16] (to allow the enzymatic sulfoxidation to occur) and the ligand occupies an optimal secondary, nonoverlapping binding site. To this end, molecular dynamics simulations and energy minimization were performed to derive the lowest-energy conformer of such a ternary complex. In the resultant structure (Figure 1B), the **2a** molecule (represented by green sticks) was found to bind to a hydrophobic pocket located at the edge of the heme-containing cavity, a few angstroms away from the bound **1a** molecule; this binding mode is additionally stabilized

(16) Henriksen, A.; Smith, A. T.; Gajhede, M. *J. Biol. Chem.* **1999**, *274*, 35005−35011.
(17) Carey, F. A.; Sundberg, R. J. *Advanced Organic Chemistry*, 3rd ed.; Plenum Press: New York, 1990; Part A, pp 71−73.

by a hydrogen bond between **2a**'s carbonyl oxygen and peptide bond's hydrogen of Gly69.[18]

Comparison of Figures 1A and 1B shows that **1a** in the binary complex is oriented differently from that in the ternary complex, i.e., that binding of **2a** in the secondary site profoundly alters the orientation of the substrate in the primary site. In particular, while **1a**'s sulfur atom in the binary HRP·substrate complex faces the oxyferryl's oxygen atom (Figure 1A), in the ternary complex it is turned away from it (Figure 1B), thus making their reaction more problematic. This difference may be partially responsible for the observed inhibition of the peroxidase-catalyzed sulfoxidation of **1a** in the presence of **2a** (Table 1).

One can also see in Figure 1B that the two lone pairs of electrons of the substrate's sulfur atom are no longer equally exposed to the attacking oxygen atom (as they are in Figure 1A). Namely, the one represented by the red stick pointing northwest is much less accessible than its counterpart pointing northeast. This explains why the peroxidase·**2a** complex is stereoselective, whereas the free enzyme is essentially not (Table 1). Finally, the use of the Cahn−Ingold−Prelog convention[17] reveals that when the attacking oxygen engages the more favorably oriented lone pair, the resultant sulfoxide has the *S* configuration. In other words, our molecular modeling analysis correctly predicts not only that the enzyme·ligand complex should be stereoselective but also the absolute configuration of the predominant product.

The affinity of **2a** toward the primary binding locus in the active site of HRP is due to a combination of hydrophobic interactions of the ligand's benzene ring and hydrogen bonds formed by the ligand's hydroxamic moiety.[9,10] The same holds true for secondary binding loci (ref 11 and above). Thus other hydrophobic hydroxamic acids should be able to play a role akin to **2a**'s. We verified this hypothesis experimentally by examining the influence of various hydroxamic acids on the initial rates and stereoselectivities of the HRP-catalyzed sulfoxidation of **1a** with *t*-BuOOH in 99.8% methanol. One can see in Table 2 that all three ring-substituted benzohydroxamic acids tested, **2b**, **2c**, and **2d**, inhibit the enzymatic formation of the *R* sulfoxide of **1a** much stronger than that of its *S* enantiomer, thus significantly increasing the stereoselectivity.[8] That **2e** with its bulky adamantane moiety is also quite potent in raising the *E*(*S*/*R*) value (sixth line in Table 2) suggests that the secondary ligand binding site (Figure 1B) is spacious and that aromatic $\pi-\pi$ interactions play no role. However, it is important for a stereoselectively boosting ligand to have a hydrophobic moiety; as seen in the penultimate line in Table 2, **2f** is virtually ineffective. Finally, having the unsubstituted hydroxamic moiety is preferable, presumably due to its greater propensity to engage in hydrogen bonding with the enzyme, for **2g** is less effective than **2a** at the same concentration (Table 2).

To ascertain the generality of the observed ligand-induced enhancement of peroxidase's stereoselectivity, we examined three additional thioethers, **1b**, **1c**, and **1d**, as sulfoxidation substrates in 99.8% methanol. In all instances, the free enzyme exhibited no appreciable stereoselectivity (*E* values in the 1.0−1.5 range). And yet, for all three prochiral substrates (Figure 2), as for **1a** (Table 1), in the presence of **2a** the enzyme was unequivocally stereoselective.

In closing, we discovered that complex formation of HRP with hydrophobic hydroxamic acids strongly enhances the stereoselectivity of enzymatic sulfoxidations. This effect was comprehensively rationalized by means of structure-based molecular modeling, providing new insights into the much-researched mechanism of ligand binding to the active site of peroxidase.

(18) It is worth mentioning that when our molecular dynamics and energy minimization approach was used to model the structures of the binary complexes of oxyferryl-HRP with **1a** (Figure 1A) and with **2a** (not shown), the substrate and the ligand were found to be located in essentially the same site. This result is in agreement with the literature X-ray crystallographic data,[10,16] thereby validating our molecular modeling methodology. The secondary binding site occupied by **2a** in the ternary complex (Figure 1B) is not as hospitable energetically as the main binding site. However, when the latter is occupied by **1a** (which is required for the peroxidase-catalyzed sulfoxidation), that secondary binding site apparently becomes the next best option, and the resultant ternary complex (Figure 1B) was found to have the lowest energy structure.

Table 2. Initial Rates and Stereoselectivties *E*(*S*/*R*) of the Asymmetric Sulfoxidation of Thioanisole (**1a**) with *t*-BuOOH Catalyzed by HRP in 99.8% Methanol in the Presence of Different Hydroxamic Acid Ligands[a]

		initial rate of product formation,[b] μM/min		
ligand	[ligand], mM	*S* sulfoxide	*R* sulfoxide	*E*(*S*/*R*)[8]
none		2.4 ± 0.3	1.3 ± 0.2	1.8 ± 0.2
2a	7.0	0.27 ± 0.03	0.046 ± 0.005	5.9 ± 0.6
2b	1.0	0.38 ± 0.02	0.066 ± 0.004	5.7 ± 0.3
2c	1.0	0.33 ± 0.02	0.058 ± 0.003	5.7 ± 0.3
2d	7.0	0.12 ± 0.02	0.028 ± 0.003	4.3 ± 0.6
2e	16	0.32 ± 0.04	0.033 ± 0.002	9.7 ± 1.0
2f	10	0.13 ± 0.01	0.052 ± 0.002	2.5 ± 0.1
2g	7.0	0.97 ± 0.02	0.24 ± 0.01	4.0 ± 0.1

[a] Lyophilized enzyme powders were suspended (at 10 mg/mL) in methanol (0.2% water) containing 0.5 mM thioether, 1 mM *t*-BuOOH, and a ligand at the highest possible concentration that still allowed measurement of the initial rate of the enzymatic production of the slower (*R*) enantiomer, except for **2g** where the ligand overlaps with the *S* sulfoxide in the HPLC chromatogram. The reaction mixtures were vigorously stirred at room temperature; periodically, aliquots were withdrawn and assayed by chiral HPLC as described in the Methods section. [b] See footnote *b* to Table 1.

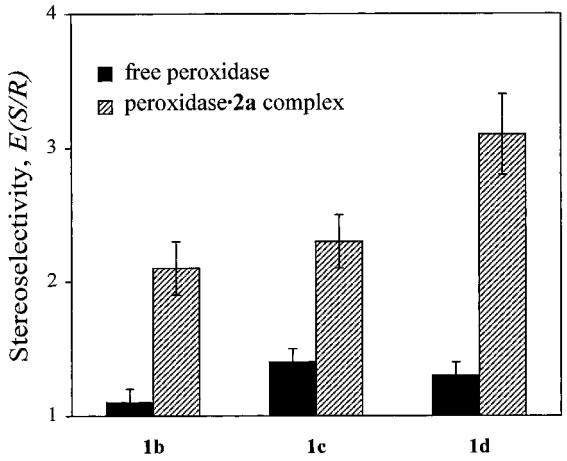

Figure 2. Stereoselectivities of HRP, in the absence and in the presence of **2a**, in the sulfoxidations of various aromatic thioethers in 99.8% methanol. Note that the *E*(*S*/*R*)[8] value of 1 (the *X*-axis) means no stereopreference. The error bars correspond to the calculated standard errors. Experimental conditions: lyophilized peroxidase powder was suspended (at 10 mg/mL) in methanol containing 0.2% water (v/v), as well as the corresponding 0.5 mM thioethers (1 mM in the case of **1c**), 1 mM *t*-BuOOH (H_2O_2 in the case of **1c**), and **2a** in the highest concentration that still allowed accurate measurement of the initial rates of the enzymatic production of the slower, *R* product enantiomer (1.0, 0.5, and 4.0 mM for **1b**, **1c**, and **1d**, respectively). The reaction mixtures were vigorously stirred at room temperature; periodically, aliquots were withdrawn and assayed by chiral HPLC. For other conditions, see the Methods section.

Materials and Methods

Materials. HRP (type II, EC 1.11.1.7) was purchased from Sigma Chemical Co. The thioether substrates **1a**−**d**, the ligands **2a**−**g**, guaiacol (*o*-methoxyphenol), and *t*-BuOOH (70% aqueous solution) were obtained from Aldrich Chemical Co. Methanol (dried by us over 3-Å molecular sieves prior to use) and H_2O_2 (30% aqueous solution) were from Mallinckrodt, and hexane and isopropyl alcohol were from EM Science. All other chemicals and solvents used were purchased from Aldrich Chemical Co., were of the highest purity available, and were used without further purification.

Enzyme Preparation. HRP was dissolved (5 mg/mL) in a 50 mM aqueous phosphate buffer (pH 7.0); then the solution was frozen with liquid N_2 and lyophilized for 48 h in a Labconco freeze-drier (−50 °C, 40−60 μm Hg). When the enzyme was lyophilized in the presence of **2a**, the latter was added to the buffered solution at a desired concentration, and the pH was adjusted to 7.0 before and after the addition of enzyme. The lyophilized enzyme powder was suspended in 99.8% (v/v) methanol containing a thioether, a peroxide, and a ligand (if any), and briefly sonicated.

Kinetic Measurements. The initial rates of the enzymatic sulfoxidation of **1a** and other thioethers with peroxides were followed by isocratic high-performance liquid chromatography (HPLC) using a Chiralcel OD-H column (4.6 mm i.d. x 250 mm). Chiral HPLC conditions (the mobile phase and flow rate) for the separation of the enantiomers of the sulfoxides produced from **1a**−**d** and the retention times for the *R* and *S* enantiomers were respectively as follows: (**1a**) 90:10 (henceforth, all such ratios are v/v) hexane/isopropyl alcohol, 0.5 mL/min, 23.0 and 30.0 min; (**1b**) 90:10 hexane/isopropyl alcohol, 0.7 mL/min, 30.2 and 38.1 min; (**1c**) 92:8:0.1 hexane/ethanol/trifluoroacetic acid, 0.5 mL/min, 45.0 and 52.0 min; and (**1d**) 92:8 hexane/isopropyl alcohol, 0.6 mL/min, 28.5 and 34.0 min. In the presence of certain hydroxamic acid ligands, HPLC conditions/retention times were distinct from those listed above for methyl phenyl sulfoxide enantiomers: (**2a**, **2d**-**2f**) 90:10 hexane/isopropyl alcohol, 0.5 mL/min, 23.0 and 30.0 min; (**2b**, **2c**) 95:5 hexane/isopropyl alcohol, 0.8 mL/min, 24.2 and 32.8 min; and (**2g**) 96:4 hexane/isopropyl alcohol, 1.1 mL/min, 22.1 and 31.0 min. The elution order for the *R* and *S* enantiomers of all sulfoxides was assumed to be that previously established[7] and confirmed[19] for their homologue methyl phenyl sulfoxide. The absorbance of the effluent was monitored at 242 nm for methyl phenyl sulfoxide and 254 nm for all other sulfoxides.

The initial sulfoxidation rates were typically measured as follows: 1 mL of 99.8% methanol containing 0.5 mM thioether (1 mM in the case of **1c**), 1 mM peroxide (2 μL of 0.5 M in water), and a desired concentration of hydroxamic acids was added to lyophilized HRP (1 mg/mL in the case of H_2O_2 and 10 mg/mL in the case of *t*-BuOOH; note that "mg" refers to the enzymic protein, i.e., after the calculated weight of the buffer salt and the ligand has been subtracted from the overall weight of the powder). The mixture was vigorously stirred at room temperature; periodically, 25-μL aliquots were withdrawn and centrifuged, 5 μL of the supernatant was analyzed by chiral HPLC, and the sulfoxide product concentration was plotted as a function of the enzymatic reaction time.

Peroxidase-catalyzed oxidation of guaiacol with H_2O_2 in 99.8% methanol was monitored spectrophotometrically at 436 nm as previously described.[20] The enzyme (0.05 mg/mL) was suspended directly in a spectrophotometric cuvette containing 3 mL of a reaction mixture consisting of 0.5 mM guaiacol, 0.1 mM H_2O_2, and a desired concentration of **2a** at room temperature.

Molecular Modeling. Molecular models of the binary HRP·**1a** and HRP·**2a** complexes and the ternary HRP·**1a**·**2a** complex were built on the basis of the published X-ray crystal structures[10,16] of HRP and its complexes by using a two-step procedure described below, similar to that[13] previously employed by us with hydrolases.

The **1a** and **2a** moieties were constructed by using standard molecular fragments provided within the INSIGHT II software (Accelrys, Princeton, NJ). The structure of HRP in its complex with ferulic acid and cyanide[16] was obtained by retrieving the heavy atom coordinates (entry 7ATJ) from the Brookhaven Protein Data Bank.[21] The ferulic acid moiety was excised, and the heme's iron-bound cyanide was replaced by an oxygen atom, thus converting the enzyme to the catalytically active compound I (an Fe═O oxyferryl species). Since solvent molecules and counterions were not included in the simulations, **1a**, **2a**, all protein residues, and the oxyferryl-heme were modeled in their un-ionized form. The coordinates of the added hydrogens were generated according to idealized bond lengths and valence angles by using the Builder module of INSIGHT II. The CVFF force field[22] provided within the FDISCOVER program (Accelrys) was used for potential and charge assignments of **1a**, **2a**, and all HRP's amino acid residues. The force field parameters and charges for the protoporphyrin IX moiety of the heme were taken from a previous cytochrome *c* study[23] and ab initio calculations[24] on model systems of cytochrome P450, respectively. The Fe═O bond distance was taken to be 1.78 Å, and a force constant of 300 kcal/mol was used.[25] The charges for the oxyferryl moiety were obtained from an ab initio CASSCF calculation on high-valent iron-oxo-porphyrins.[26]

To model the oxyferryl-peroxidase·**1a** complex, the **1a** molecule was placed in the substrate binding site of HRP, which in the X-ray crystal structure[16] is occupied by ferulic acid. First, this initial structure was energy-minimized to relieve any overlay-strained artifacts using the steepest descent method for 500 iterations or until the RMS gradient fell below 0.1 kcal/Å, followed by the conjugate-gradient minimization until the maximum derivative dropped below 0.01 kcal/Å. For subsequent calculations, the sulfur-bonded carbon of **1a**'s phenyl ring was tethered by using a harmonic potential (see below); this carbon atom was selected because its coordinates virtually coincide with the centers of both mass and geometry of the substrate. The purpose of the tethering was to allow widely different conformations to be explored while preventing the substrate from diffusing too far from the enzyme. The energy-minimized structure was then subjected to 1000 steps of molecular dynamics simulation at 900 K using the Verlet leapfrog integrator with a step size of 1 fs and a template harmonic force of 2 kcal/Å. After each simulated ps, the resulting structure was energy-minimized as outlined above, except that the maximum derivative for the conjugate gradient method was set to be less than 0.005 kcal/Å and a template forcing constant of 0.2 kcal/Å was used. The coordinates of the minimized structure were then saved, and its energy was calculated. This cycle was repeated until 100 energy-minimized structures were obtained; four lowest energy ones of them were chosen for further analysis.

Second, each of the four lowest energy conformers thus identified was used as an initial model for a new set of dynamics/minimization calculations. The procedure was the same as described in the preceding paragraph, except that the initial optimization was omitted. The cycle was repeated until 125 structures of each lowest energy conformer were obtained; the resultant total of 500 energy-minimized structures was

(19) Colonna, S.; Gaggero, N.; Carrea, G.; Pasta, P. *J. Chem. Soc., Chem. Commun.* **1992**, 357−358.
(20) Dai, L.; Klibanov, A. M. *Proc. Natl. Acad. Sci. U.S.A.* **1999**, *96*, 9475−9478.
(21) Berman, H. M.; Westbrook, J.; Feng, Z.; Gilliland, G.; Bhat, T. N.; Weissig, H.; Shindyalov, I. N.; Bourne, P. E. *Nucleic Acid Res.* **2000**, *28*, 235−242.
(22) Dauber-Osguthorpe, P.; Roberts, V. A.; Osguthorpe, D. J.; Wolff, J.; Genest, M.; Hagler, A. T. *Proteins* **1988**, *4*, 31−47.
(23) Laberge, M.; Vanderkooi, J. M.; Sharp, K. A. *J. Phys. Chem.* **1996**, *100*, 10793−10801.
(24) de Groot, M. J.; Havenith, R. W. A.; Vinkers, H. M.; Zwaans, R.; Vermeulen, N. P. E.; van Lenthe, J. H. *J. Comput.-Aided Mol. Des.* **1998**, *12*, 183−193.
(25) Paulsen, M. D.; Ornstein, R. L. *J. Comput.-Aided Mol. Des.* **1992**, *6*, 449−460.
(26) Yamamoto, S.; Teraoka, J.; Kashiwagi, H. *J. Chem. Phys.* **1988**, *88*, 303−312.

collected, and their energies were calculated. Finally, the single lowest energy conformer obtained overall was chosen as that representing the catalytically relevant oxyferryl-HRP·**1a** complex (Figure 1A).

During all simulations, nonbonded interactions were evaluated with a group-based switching function between 23 and 25 Å, and the nonbonded pair list was updated every 10 time steps. Only the atoms of the substrate, of the oxyferryl-heme, and of the amino acid residues within HRP's heme cavity (Arg38, Phe41, His42, Phe68, Gly69, Asn70, Ala71, Asn72, Ser73, Leu138, Pro139, Ala140, Pro141, Phe142, Phe143, and Phe179) were allowed to move. Neither cross-terms nor Morse functions were used, and the dielectric constant of the medium was set to 4.0.

To model the ternary HRP·**1a**·**2a** complex, we had to identify where **2a** is bound within the enzyme when the main binding site is occupied by **1a**. A previous theoretical study of binding modes of **2a** in HRP[11] has shown that, in addition to the main substrate binding site,[10,16] **2a** can also be accommodated in several other loci regarded as secondary binding sites. The first such putative secondary binding site[11] is located at the proximal side of the heme more than 10 Å from the main binding site. In this location, **2a** is surrounded by Phe68, Pro141, Phe142, Arg178, Phe179, Ile180, Met181, Asp182, Phe187, Ser188, Ile244, and Gln245. The other secondary binding site was identified during our analysis of the molecular dynamics trajectories of the binary HRP·**1a** complex, whereby it was observed that **1a** is transiently accommodated in a pocket adjacent to the main binding site. When **2a** is docked in that secondary site, it is surrounded by **1a** and Asp66, Ala67, Phe68, Gly69, Asn70, Ala71, Asn72, Ser73, Pro141, Gln176, Arg178, and Phe179 residues of the enzyme.

The coordinates of the lowest energy conformer obtained from the simulation of the binary HRP·**1a** complex were used as the basis for the modeling of the ternary HRP·**1a**·**2a** complex. The ligand was manually docked into both aforementioned secondary binding sites; the coordinates of the two structures thus generated were saved and used as the input for the subsequent simulations. The two-step procedure used here was analogous to that described for the binary enzyme·**1a** complex, except that **2a** and the amino acid residues of the enzyme that surround both binding sites were also allowed to move during the simulations. The lowest energy conformer for each secondary binding site was identified, and it was found that the conformation of the ternary complex with **2a** neighboring the main binding site was 2.0 kcal/mol more stable than the other.[11] Therefore, the structure in which **2a** is bound to the enzyme in the vicinity of **1a** was chosen as the catalytically relevant conformation of the ternary HRP·**1a**·**2a** complex (Figure 1B).

Finally, to verify our computational techniques, we applied them to model the structure of the previously solved[10] HRP·**2a** complex. To that end, **2a** was placed in three different locations within the free enzyme: the main substrate binding site, and the two secondary binding sites used for the modeling of the ternary complex. The three initial structures generated were saved and employed as the input for subsequent simulations by using the same procedure as that described for modeling the ternary complex. When the lowest energy conformers of each simulation were selected, they revealed that the energetically preferred binding site for **2a** in HRP is the main binding site, which is indeed the one experimentally identified by the X-ray crystallographic analysis.[10]

Acknowledgment. This study was financially supported by grant no. BES-9712497 from the National Science Foundation. J.M.M.C. is a recipient of a postdoctoral fellowship from the Spanish Ministry of Education, Culture, and Sports.

JA012075O